

Received November 22, 2017, accepted December 30, 2017, date of publication January 23, 2018, date of current version March 13, 2018.

Digital Object Identifier 10.1109/ACCESS.2018.2796579

# Memory-Full Context-Aware Predictive Mobility Management in Dual Connectivity 5G Networks

ABDELRAHIM MOHAMED<sup>1</sup>, (Member, IEEE), MUHAMMAD ALI IMRAN<sup>2</sup>, (Senior Member, IEEE), PEI XIAO<sup>1</sup>, (Senior Member, IEEE), AND RAHIM TAFAZOLLI<sup>1</sup>, (Senior Member, IEEE)

<sup>1</sup>Institute for Communication Systems, Home of 5GIC, University of Surrey, Guildford GU2 7XH, U.K.

<sup>2</sup>School of Engineering, University of Glasgow, Glasgow G12 8QQ, U.K.

Corresponding author: Abdelrahim Mohamed (abdelrahim.mohamed@surrey.ac.uk)

This work was supported in part by the U.K. Engineering and Physical Sciences Research Council (EPSRC) under Grant EP/R001588/1 and in part by the EPSRC Global Challenges Research Fund through the DARE Project under Grant EP/P028764/1.

**ABSTRACT** Network densification with small cell deployment is being considered as one of the dominant themes in the fifth generation (5G) cellular system. Despite the capacity gains, such deployment scenarios raise several challenges from mobility management perspective. The small cell size, which implies a small cell residence time, will increase the handover (HO) rate dramatically. Consequently, the HO latency will become a critical consideration in the 5G era. The latter requires an intelligent, fast, and light-weight HO procedure with minimal signaling overhead. In this direction, we propose a memory-full context-aware HO scheme with mobility prediction to achieve the aforementioned objectives. We consider a dual connectivity radio access network architecture with logical separation between control and data planes because it offers relaxed constraints in implementing the predictive approaches. The proposed scheme predicts future HO events along with the expected HO time by combining radio frequency performance to physical proximity along with the user context in terms of speed, direction, and HO history. To minimize the processing and the storage requirements whilst improving the prediction performance, a user-specific prediction triggering threshold is proposed. The prediction outcome is utilized to perform advance HO signaling whilst suspending the periodic transmission of measurement reports. Analytical and simulation results show that the proposed scheme provides promising gains over the conventional approach.

**INDEX TERMS** Context awareness, control/data separation architecture, memory-full networking, mobility management.

## I. INTRODUCTION

The ambitious capacity and performance targets of the fifth generation (5G) cellular system motivated academic, industrial and standardisation bodies to identify three main themes for the 2020 era. These include network densification with massive deployment of small cells, spectrum aggregation with wider allocations at high frequency bands, and multiple-input multiple-output (MIMO) antenna systems with improved spectral efficiency [1], [2]. Since the propagation path loss increases dramatically at high frequency bands, the latter can only be used in local area and small cell deployment scenarios. In other words, network densification and spectrum extension are highly correlated and they share the same deployment theme: small cells. Despite the potential gains, mobility management becomes complex in such scenarios, and the conventional approaches may not be suitable from

signalling load, monitoring overhead and handover (HO) latency perspectives.

Typically, any cellular system includes a network and mobile devices, where the former consists of a core-network and a radio access network (RAN). In cellular terminology, the RAN consists of several base stations (BSs) that transmit/receive data and control signals to/from the mobile devices over the air interface. The users camp on the network by selecting the BS that offers the highest signal strength (SS) and/or signal quality (SQ). When the users move, the SS/SQ of the serving BS degrades while the SS/SQ of a neighbouring BS(s) increases. This results in a cell reselection operation (if the user is in the idle mode) or a HO operation (if the user is in the active mode).

Such an operation requires the user equipment (UE), i.e., the mobile device, to continuously monitor SS/SQ of the serving and the neighbouring BSs. The monitoring is

performed at measurement gaps during which the UE cannot transmit/receive data. For instance, with a measurement gap periodicity of 200 ms the UE suspends the data transmission/reception every 200 ms. In dense deployment scenarios, the rate of change in SS/SQ measurements will be higher than in current systems due to the smaller cell size and the large number of available candidates. A fast tracking of this behaviour requires increasing the measurement gap periodicity. In addition, a longer measurement gap may be required when there are several candidate BSs to be monitored (i.e., in dense deployment scenarios) or when the neighbouring BSs are operating in several portions of the spectrum. These enhancements for SS/SQ monitoring could come at the expense of reducing the achievable data rate and degrading the quality-of-service (QoS) because more time domain resources are being reserved for the monitoring process without being used for data transmission.

At the signalling dimension, the cell reselection process is mobility-friendly, since cell reselection is performed by the UE without (or with a minimal) signalling exchange. The rationale to maintain the reselection decision at the UE side can be justified since the reselection process does not require resource release at the source BS or resource assignment at the target BS. On the other hand, the HO process requires signalling exchange in a fast, reliable and accurate manner to avoid service disruption. Each HO includes a decision phase where the target BS is determined, a preparation phase where the source and the target BSs exchange the UE parameters and allocate the radio resources, an execution phase where the UE disconnects from the source BS and accesses the target BS, and a completion phase where the data plane path at the core-network is switched towards the target BS. These phases require multiple signalling exchange as follows.

- Signalling exchange between the UE and the serving BS.
- Signalling exchange between the UE and the target BS.
- Signalling exchange between the serving BS and the target BS.
- Signalling exchange between the serving/target BS and the core-network.

This procedure is triggered for each HO, thus the signalling load increases linearly with the number of HOs. Since the HO rates are expected to increase significantly in dense deployment scenarios, the associated signalling load may increase dramatically. In this regard, the overhead could degrade the performance in both the RAN side and the core-network side.

From the latency perspective, the small cell size requires fast HO procedures to ensure a successful HO. The latter can be achieved only when the SS/SQ stays above a certain threshold during the HO process, see [3] for the HO success/failure conditions. Based on current standards such as the long term evolution (LTE), the overall HO latency is in the range of 100–200 ms which is sufficient for the current density levels. Due to the high SS/SQ rate of change in dense deployment scenarios, a faster and light-weight procedure is required to ensure that the HO process is completed before the success/failure threshold is reached.

In this paper, we tackle these challenges by proposing a predictive mobility management scheme that predicts future HO events along with the expected HO time to enable fast and advance signalling exchange with minimal overhead and latency in dense deployments scenarios. A futuristic dual connectivity RAN architecture with logical separation between control and data planes is considered due to its unique features and intrinsic signalling-efficient design. The proposed scheme includes short-term and long-term memories, and it combines radio frequency (RF) performance to physical proximity along with the UE contextual information in terms of speed, direction and HO history. To minimise the processing and the storage requirements whilst improving the prediction and HO performance, a user-specific prediction triggering threshold is proposed. A switching criteria between advance and conventional HO signalling is defined, resulting in a predictive HO scheme with two operation modes. Analytical and system level simulation results show promising gains of the proposed scheme over the conventional approach.

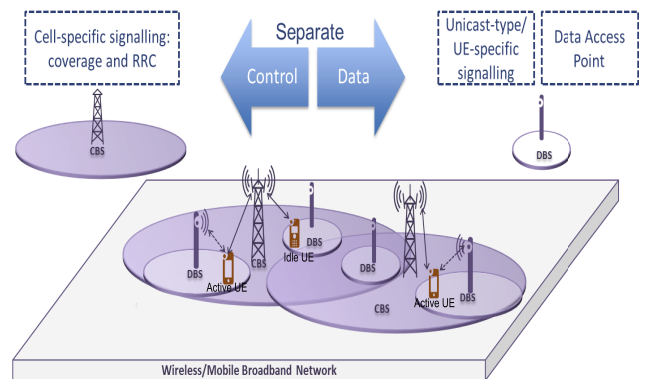


FIGURE 1. Dual Connectivity RAN with control/data plane separation.

The remainder of this paper is structured as follows: Section II describes the network architecture and presents the main components of the proposed scheme. Section III develops the prediction model utilising a memory-full approach, while Section IV models the context-aware units to aid the prediction outcome and the HO decision. Section V presents and discusses numerical and simulation results. Finally, Section VI concludes the paper.

## II. NETWORK ARCHITECTURE AND PROPOSED SCHEME

We propose a memory-full context-aware HO scheme with mobility prediction and advance signalling to achieve a light-weight, signalling-efficient and fast HO procedure. We consider the dual connectivity RAN architecture with control/data plane separation [4] as it has been identified by the third generation partnership project (3GPP) as one of the candidate 5G RAN features [5]. Fig. 1 shows a high level overview of this architecture. It consists of a control base station (CBS) layer and a data base station (DBS) layer. The former is formed of macro BSs deployed at low frequency bands to provide ubiquitous connectivity, while the latter is

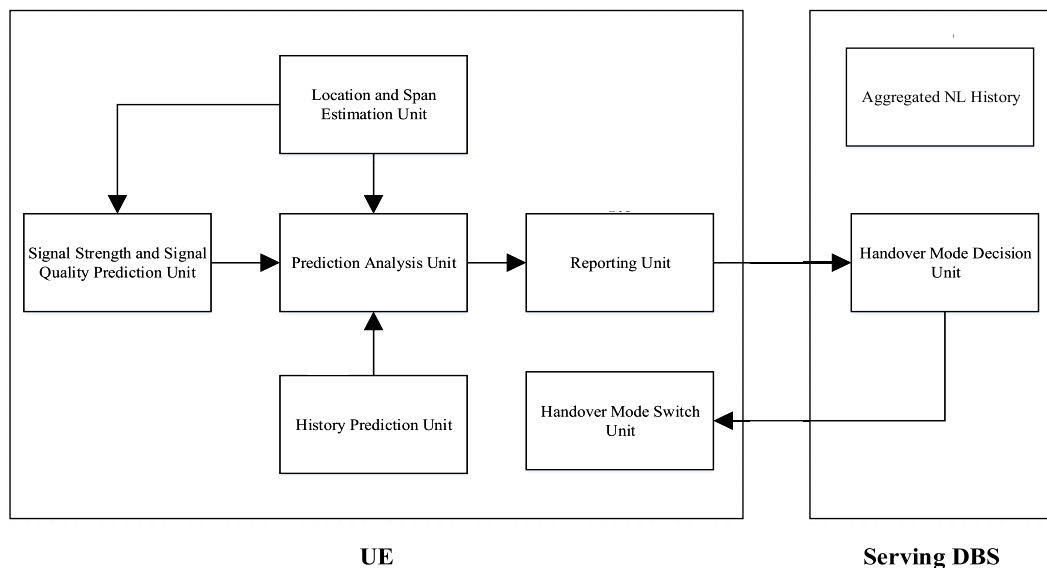


FIGURE 2. System model of the memory-full context-aware predictive handover scheme.

formed of small BSs deployed at high (or low) frequency bands to provide on-demand high data rate transmission. The control/data separation architecture (CDSA) requires the active UE to maintain a dual connection with both the CBS and the DBS, while idle UE (and detached UE accessing the network) maintains a single connection with the CBS only [4], [6], [7]. The DBS is invisible to both detached and idle UE, and its on-demand connection with the active UE is established and assisted by the CBS.

The dual connection feature of the CDSA coupled with contextual information enable implementing fast and predictive HO schemes at the DBS layer. Predicting the UE mobility (at DBS level rather than the exact location) allows the source and the candidate DBSs to prepare and reserve resources in advance, which in turn could simplify the HO process and minimise the associated monitoring overhead, RAN signalling and interruption time [8], [9]. In the conventional RAN architecture, the predictive strategies have tight constraints since an incorrect prediction with a break-before-make HO can lead to detaching the UE from the network. In other words, an incorrect prediction in the conventional RAN does not only increase the HO latency and signalling overhead, but also it requires a new UE-network connection establishment. On the other hand, the CDSA offers relaxed constraints in implementing predictive HO management strategies. An incorrect DBS prediction in the CDSA does not require UE-network connection re-establishment, since the UE maintains another low rate connection with the CBS. In this direction, we propose predictive mobility management at DBS-level under the CDSA architecture.

The proposed scheme depends on DBS SS and/or SQ prediction performed by the UE. This prediction is aided by UE context information such as location, direction and speed, in addition to statistical information based on either the UE HO history or the aggregated per-DBS Neighbour List (NL)

HO history. A short-term memory for the RF measurements and a long-term memory for the HO history are considered, hence we describe this scheme as a memory-full context-aware mobility management approach. The predicted DBS is reported on an event basis to the serving (i.e., the source) DBS, which determines the reporting criteria and the HO mode to be followed by the UE. The prediction process is triggered only once when a certain prediction triggering threshold is reached. As shown in Fig. 2, the memory-full context-aware predictive DBS HO scheme comprises a location and span estimation unit, a SS and SQ prediction unit, a history prediction unit, a prediction analysis unit, a reporting unit, a HO mode decision unit and a HO mode switch unit.

The UE periodically measures SS and SQ of the serving DBS and the top- $m$  other detectable DBSs at every measurement gap as in current standards. The 3GPP Measurement Reporting and Control (MRC) [10] may be re-used as an example of this measurement and optional reporting mechanism. The reported strongest or best quality DBSs are limited to  $m$  per DBS categorisation as the measurement interval is limited and measurement power consumption and normal transmission need to be balanced against the accurate measurement report (MR) cycle. The SS and SQ prediction unit stores measurements of a subset of the top- $m$  detectable DBSs that reside within the angular span of the UE direction/speed. The location and span estimation unit triggers the prediction process when the UE reaches the inner edge of cell (EoC) boundary of the serving DBS. The latter can be defined based on a distance threshold or a SS/SQ threshold. When the prediction is triggered, the SS and SQ prediction unit uses the stored measurements to predict SS and/or SQ of the serving DBS and the candidate DBSs.

The prediction analysis unit evaluates the predicted SS/SQ to determine if a certain DBS HO criteria is satisfied. If the

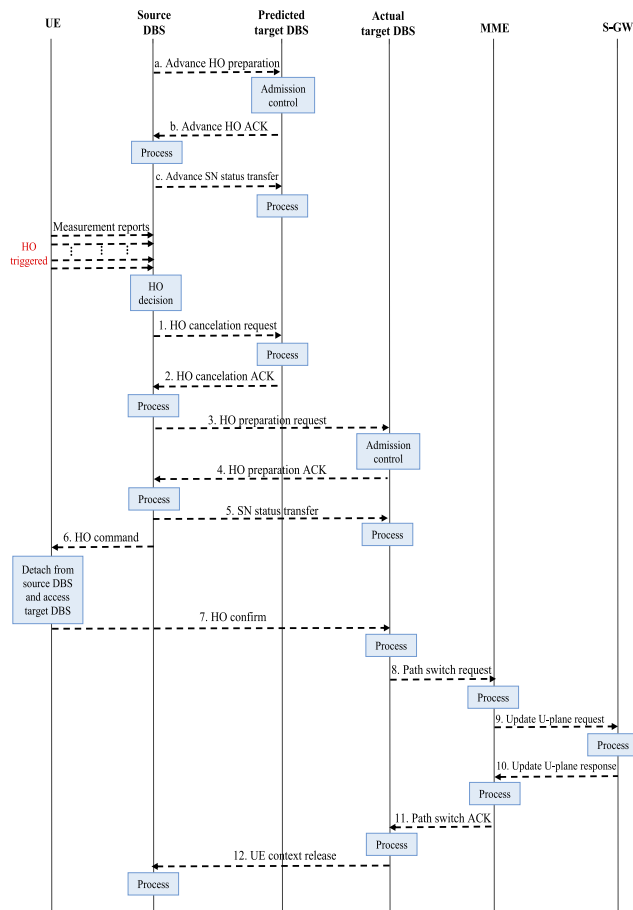


**FIGURE 3. Signalling flow diagram for predictive and non-predictive HO scenarios, based on the LTE X2 HO procedure. Signalling messages in non-predictive HO: 3, 4, 5, 6, 7, 8, 9, 10, 11, 12. Signalling messages in predictive HO with correct prediction (Network decision): 6, 7, 8, 9, 10, 11, 12. Signalling messages in predictive HO with correct prediction (HO control delegated to UE): 7, 8, 9, 10, 11, 12. Signalling messages in predictive HO with incorrect prediction: 1, 2, 3, 4, 5, 6, 7, 8, 9, 10, 11, 12. Acronym ACK: Acknowledgement, SN: Sequence Number. Notice that the HO hysteresis is not shown here because it is applied before the signalling exchange.**

predicted SS and/or SQ of a neighbouring DBS meets the HO criteria, then the prediction analysis unit queries the history prediction unit. The latter provides the prediction analysis unit with the probability of successful HO based on either the UE HO history or the DBS aggregated HO history. Based on these metrics as well as the predicted HO time, the prediction analysis unit may command the reporting unit to generate a new light-weight report called predictive measurement report (PrMR) and sends it to the serving DBS. This PrMR is sent only once as opposed to the periodic MR transmission in the conventional HO approach. At the serving DBS side, the HO mode decision unit evaluates the PrMR and commands the UE to operate either in a predictive mode or revert back to the conventional non-predictive mode. In the former case, the conventional MR is suspended, the HO-related RAN signalling is performed in advance and HO control is delegated to the UE. On the other hand, the non-predictive mode follows the conventional HO procedure where the HO decision

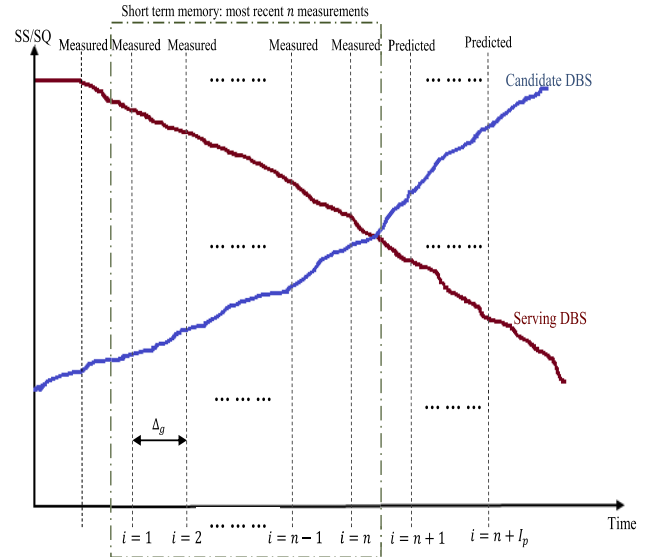


**FIGURE 4. Exemplary operation of the signal strength and signal quality prediction unit.**

is taken by the serving DBS after the HO criteria is met. Fig 3 shows a signalling flow diagram for the HO process based on the LTE X2 HO approach. The operation, algorithms and interactions of the proposed units are formulated and described in the following sections.

### III. MEMORY-FULL PREDICTION UNITS

#### A. SIGNAL STRENGTH/QUALITY PREDICTION

Fig. 4 shows an exemplary operation of the SS and SQ prediction unit. It contains a short-term memory that stores the most recent  $n$  active state measurements of the DBSs that reside within the angular span of the UE direction/speed. In other words, the SS/SQ prediction window size is  $n$  measurements per DBS. The SS/SQ prediction is based on measurement trends. To minimise the UE storage requirements and remove signal fading/fluctuation effects, Grey system theory [11] is adopted as the trending approach. The Grey theory has been used in several fields, e.g., for disaster, season and sequence prediction. It requires limited amount of input data and implicitly averages this data. The basic concept depends on translating the data sequence into a monotonic increasing function, representing this function by a differential equation and solving it to find the model's parameters. For the problem under study (i.e., SS/SQ prediction), a  $GM(1,1)^1$  Grey model [11] can be constructed for each DBS as:

- The original SS/SQ measurements stored in the short-term memory are represented as a time series given by

$$y^{(0)}(i) = (y^{(0)}(1), y^{(0)}(2), \dots, y^{(0)}(n)) \quad (1)$$

where the superscript  $(0)$  means original SS/SQ measurements (i.e., before processing) and  $i = 1, 2, 3, \dots, n$  is the measurement index.

<sup>1</sup>the first 1 means the model uses first order differential equations, while the second 1 means there is one variable.

- An accumulated generating operation (AGO) translates  $y^{(0)}(i)$  to a monotonic increasing function  $y^{(1)}(i)$  as

$$y^{(1)}(i) = \text{AGO} \left\{ y^{(0)}(i) \right\} = \left( y^{(0)}(1), \sum_{i=1}^2 y^{(0)}(i), \dots, \sum_{i=1}^n y^{(0)}(i) \right). \quad (2)$$

- Based on (2), an inverse accumulated generating operation (IAGO) can be formulated as

$$y^{(1)}(i) = y^{(1)}(i - 1) + y^{(0)}(i). \quad (3)$$

- The GM(1,1) model is defined by the following equation:

$$\frac{dy^{(1)}}{du} + ay^{(1)} = b \quad (4)$$

where  $a$  is the development parameter and  $b$  is the grey input. The solution to (4) at time index  $i$  is

$$y^{(1)}(i + 1) = \left( y^{(1)}(1) - \frac{b}{a} \right) e^{-ai} + \frac{b}{a} = \left( y^{(0)}(1) - \frac{b}{a} \right) e^{-ai} + \frac{b}{a}. \quad (5)$$

By substituting the IAGO of (3) into (5), the predicted SS/SQ one measurement gap in advance  $y_p^{(0)}(i + 1)$  can be expressed as

$$y_p^{(0)}(i + 1) = e^{-ai} (1 - e^a) \left( y^{(0)}(1) - \frac{b}{a} \right). \quad (6)$$

Similarly, the predicted SS/SQ  $j$  measurement gaps in advance can be formulated as

$$y_p^{(0)}(i + j) = e^{-a(i+j-1)} (1 - e^a) \left( y^{(0)}(1) - \frac{b}{a} \right). \quad (7)$$

Equation (7) can be used to predicted a series of SS/SQ measurements. However, the model parameters  $a$  and  $b$  need to be calculated before the prediction is performed. These parameters can be obtained by expressing the derivative in (4) as

$$\frac{dy^{(1)}}{du} \rightarrow y^{(1)}(i + 1) - y^{(1)}(i) \quad (8)$$

and the right hand side of (8) can be replaced with  $y^{(0)}(i + 1)$  based on the IAGO of (3), i.e.,

$$\frac{dy^{(1)}}{du} \rightarrow y^{(0)}(i + 1). \quad (9)$$

The mean value of adjacent SS/SQ measurements is

$$z^{(1)}(i) = \frac{1}{2} y^{(1)}(i) + \frac{1}{2} y^{(1)}(i - 1) \rightarrow y^{(1)}(u). \quad (10)$$

Based on (9) and (10), the Grey differential equation of (4) can be rewritten as

$$y^{(0)}(i) + az^{(1)}(i) = b. \quad (11)$$

Rearranging (11) and writing the resultant equation in a matrix form yields

$$\begin{bmatrix} y^{(0)}(2) \\ y^{(0)}(3) \\ \vdots \\ y^{(0)}(n) \end{bmatrix} = \begin{bmatrix} -z^{(1)}(2) & 1 \\ -z^{(1)}(3) & 1 \\ \vdots & \vdots \\ -z^{(1)}(n) & 1 \end{bmatrix} \cdot \begin{bmatrix} a \\ b \end{bmatrix}. \quad (12)$$

Finally,  $a$  and  $b$  can be obtained by solving (12), i.e.,

$$\begin{bmatrix} a \\ b \end{bmatrix} = \begin{bmatrix} -z^{(1)}(2) & 1 \\ -z^{(1)}(3) & 1 \\ \vdots & \vdots \\ -z^{(1)}(n) & 1 \end{bmatrix}^{-1} \cdot \begin{bmatrix} y^{(0)}(2) \\ y^{(0)}(3) \\ \vdots \\ y^{(0)}(n) \end{bmatrix}. \quad (13)$$

The SS and SQ prediction unit uses this model to predict SS and SQ of the serving DBS and a subset of the top- $m$  other detectable DBSs. These results are fed to the prediction analysis unit. It is worth mentioning that other trending techniques, such as polynomial fitting or sample extrapolation, can be used instead of the Grey model.

The expected HO time can be predicted based on the rate of SS/SQ degradation. The measurement prediction is performed in time domain and on a sample-basis. Thus if the measurement gap  $\Delta_g$  is constant (such as in current standards), the SS and SQ prediction unit predicts a series of measurements until the HO criteria is satisfied (see Fig. 4). For example, if the prediction is performed for  $I_p$  samples in advance (i.e., assuming that the current measurement index is  $n$ , and the predicted SS/SQ that satisfies the HO criteria has index  $n + I_p$ ), then the predicted remaining time for HO is

$$\text{Predicted HO time} = I_p \cdot \Delta_g. \quad (14)$$

### B. HISTORY PREDICTION

The history prediction unit provides statistical historical information based on a long-term memory that helps the prediction analysis unit to confirm or reject the measurement-based HO prediction. It calculates the HO probability from the serving DBS to the predicted DBS based on either the aggregated NL HO history [12], [13] or the UE HO history. The former is already available in current standards at the network side in the form of a HO frequency table, and it provides statistical information based on the crowd behaviour. Table 1 provides an illustrative example of the NL HO history in a table format, where  $C_{i,j}$  is the NL-based aggregated HO count from DBS <sub>$i$</sub>  to DBS <sub>$j$</sub> . Typically, each row in Table 1 is maintained by the source DBS. This NL HO history can be translated into a transition probability. For instance, the NL-based transition probability  $t_{i,j}$  from DBS <sub>$i$</sub>  to DBS <sub>$j$</sub>  can be obtained by

$$t_{i,j} = \sum_{u, \forall u \in \mathbb{N}_i} \frac{C_{i,j}}{C_{i,u}} \quad (15)$$

where  $\mathbb{N}_i$  is the neighbour list of DBS <sub>$i$</sub> , i.e., a set of all the DBSs that are neighbours to DBS <sub>$i$</sub> .

TABLE 1. Aggregated handover history in the long-term memory.

| From             | To               |                  |     |                  |                  |
|------------------|------------------|------------------|-----|------------------|------------------|
|                  | DBS <sub>a</sub> | DBS <sub>b</sub> | ... | DBS <sub>k</sub> | DBS <sub>l</sub> |
| DBS <sub>a</sub> | 0                | $C_{a,b}$        | ... | $C_{a,k}$        | $C_{a,l}$        |
| DBS <sub>b</sub> | $C_{b,a}$        | 0                | ... | $C_{b,k}$        | $C_{b,l}$        |
| ...              | ...              | ...              | ... | ...              | ...              |
| DBS <sub>k</sub> | $C_{k,a}$        | $C_{k,b}$        | ... | 0                | $C_{k,l}$        |
| DBS <sub>l</sub> | $C_{l,a}$        | $C_{l,b}$        | ... | $C_{l,k}$        | 0                |

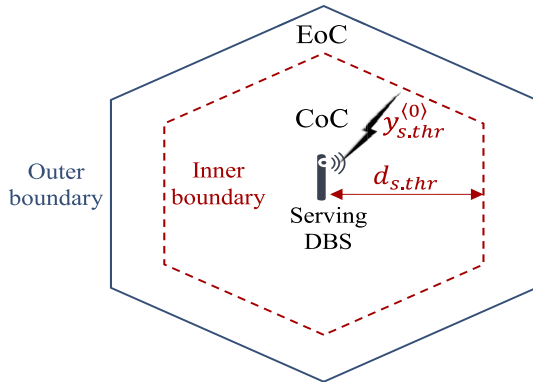


FIGURE 5. UE location estimation and CoC/EoC prediction triggering threshold.

The NL-based history can be used for DBSs covering areas characterised by high batch HO rates. For example, where multiple UE on a train perform simultaneous HOs. However, the NL-based approach may not be suitable for individual users since it provides a coarse and less accurate estimate based on the crowd behaviour. This suggests a UE-based approach where individual users maintain separate statistical information based on their own history. This can be achieved by maintaining HO history tables as in Table 1 for each user, i.e.,  $t_{i,j}$  is computed for each user based on their own  $C_{i,j}$  values, or alternatively  $t_{i,j}$  can be computed by using our online history-based prediction scheme in [9].

#### IV. CONTEXT-AWARE ASSISTANCE UNITS

##### A. LOCATION AND SPAN ESTIMATION

The main objective of this unit is minimising the UE processing load and storage requirements. The prediction process in Section III-A can be continuously executed until a target DBS is found. However, such a continuous operation may not be feasible from battery and processing perspectives. A more practical design approach is to trigger the prediction process when a certain triggering criteria is satisfied. This suggests a two boundary DBS cell structure, where the prediction is triggered at the inner boundary while the actual HO is performed at the outer boundary. Fig. 5 shows two approaches that can be used by the location and span estimation unit to trigger the prediction process at the inner boundary, based on the UE location w.r.t. the serving DBS, i.e., centre of cell (CoC) or EoC. Notice that the CoC/EoC classification is based on the inner boundary.

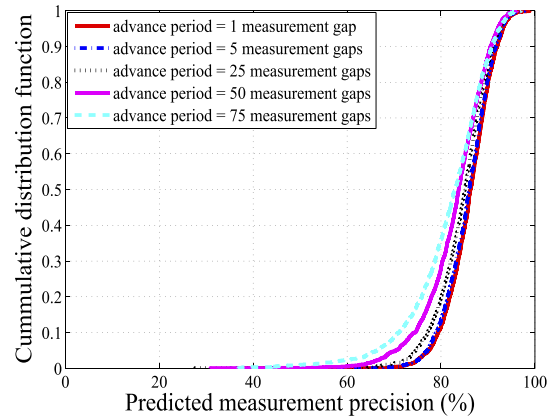


FIGURE 6. Predicted measurement precision with several advance periods, 5 UE per DBS,  $V = 10$  km/hr.

These approaches include position-based distance calculation and serving DBS signal measurements. The former requires the serving DBS to broadcast its location, e.g., in the form of longitude and latitude. Then, the distance between the UE and the serving DBS can be calculated based on the UE position (provided by either a GPS or other positioning techniques). When this distance equals to or greater than a certain threshold  $d_{s,thr}$  and it is increasing, then the UE location is EoC and the prediction process is triggered. The second approach, i.e., the serving DBS signal measurements, utilises the measured SS/SQ from the serving DBS to trigger the prediction process. When the serving DBS SS/SQ drops below a certain threshold  $y_{s,thr}^{(0)}$ , then the UE location is EoC and the prediction process is triggered.

An appropriate setting of  $d_{s,thr}$  and/or  $y_{s,thr}^{(0)}$  is of vital importance in improving the performance of the proposed scheme. A large  $d_{s,thr}$  (i.e., low  $y_{s,thr}^{(0)}$ ) setting may result in a too late prediction, i.e., the HO may happen before the prediction process is triggered. On the other hand, a small  $d_{s,thr}$  (i.e., high  $y_{s,thr}^{(0)}$ ) setting may lead to a too early prediction. This in turn increases the error probability, due to the large gap between the time when the prediction is performed and the time when the actual HO happens. In addition, radio channel and/or UE direction will have a higher changing probability when the actual HO happens. As an illustrative example, Fig. 6 shows simulation results for the measurement prediction precision with several prediction advance periods. As can be noticed, the prediction of the  $i^{th}$  SS/SQ measurement is more accurate than the prediction of the  $j^{th}$  SS/SQ measurement, where  $i < j$ .

Assuming a constant speed  $V$  and a hysteresis-based HO criteria, i.e., the HO happens if the following condition is true:

$$\log(y_n^{(0)}) \geq \log(y_s^{(0)}) + \log(\Theta) \quad (16)$$

where  $y_s^{(0)}$  and  $y_n^{(0)}$  are the SS/SQ of the serving and the neighbouring DBSs, respectively,  $\Theta$  is the HO hysteresis, and the parameters in (16) are in the linear scale. A HO hysteresis needs to be applied to the trend to ensure that

prevailing conditions only are acted upon to avoid HO ping-pong. For a general path loss model  $\chi \mathcal{R}^\xi$ , where  $\chi$  is the distance-independent path loss component,  $\mathcal{R}$  is the distance between the Tx and the Rx, and  $\xi$  is the path loss exponent. Then it can be proved that the actual HO happens after  $I_p$  measurements referenced to the prediction triggering point, where  $I_p$  is expressed as

$$I_p = \frac{\left( \left( \frac{q_s \Theta}{q_n} \right)^{\frac{1}{\xi}} \left( \frac{\psi - d_{s,thr} \cos(\phi_s)}{\cos(\phi_n)} \right) \right) - d_{s,thr}}{V \Delta_g \left( 1 + \left( \frac{\cos(\phi_s)}{\cos(\phi_n)} \right) \left( \frac{q_s \Theta}{q_n} \right)^{\frac{1}{\xi}} \right)} \quad (17)$$

where  $q_s$  and  $q_n$  are the transmit power of the serving and the neighbouring DBSs, respectively,  $\psi$  is the inter-site distance,  $\phi_s$  is the angle between the line connecting the DBSs and the line connecting the serving DBS with the UE location when the HO happens,  $\phi_n$  is the angle between the line connecting the DBSs and the line connecting the neighbouring DBS with the UE location when the HO happens. It can be noticed that (17) depends on the UE speed. Thus using a DBS-based unified triggering threshold for all users implies that different users will have different  $I_p$  values. In other words, if the prediction is triggered at the same location for all users, then low speed users will have to predict more measurements than high speed users. This may increase the error probability and decrease the prediction precision as shown in Fig. 6. This suggests a UE-specific prediction triggering threshold  $d_{s,thr,UE}$  that takes into account network parameters as well as UE parameters. This threshold can be obtained by solving (17) for  $d_{s,thr}$ , i.e.,

$$d_{s,thr,UE} = \frac{\left( \frac{q_s \Theta}{q_n} \right)^{\frac{1}{\xi}} \left( \frac{\psi - I_p V \Delta_g \cos(\phi_s)}{\cos(\phi_n)} \right) - I_p V \Delta_g}{1 + \left( \frac{\cos(\phi_s)}{\cos(\phi_n)} \right) \left( \frac{q_s \Theta}{q_n} \right)^{\frac{1}{\xi}}}. \quad (18)$$

The UE angular span is utilised to narrow down the candidate DBS set. A high speed user usually has a smaller span (i.e., probability of changing the direction is small) as compared with a low speed user. This allows the former to store and process measurements of a smaller number of DBSs as compared with the latter. The location and span estimation unit calculates the UE angular span  $\Omega$  by

$$\Omega = 2\pi e^{-\eta V} \quad (19)$$

where  $\eta$  is the span gradient. Different DBSs can define different values for  $\eta$  which can be learned from the users' behaviour. For instance, a highway DBS may define a large gradient which results into a small span (i.e., a low mobility in a highway may be attributed to traffic conditions rather than to a direction change intention). A new span is defined when the UE changes its speed abruptly, when the UE changes its direction by an angle larger than the initial span, or at regular time intervals. Based on the location of the top- $m$  detectable DBSs, the location and span estimation unit selects the DBSs

that reside within the UE span as candidates for the prediction process and store their measurements in the short-term memory. This result is fed to the SS and SQ prediction unit.

## B. PREDICTION ANALYSIS AND HANDOVER MODE DECISION

The prediction analysis unit evaluates the predicted SS/SQ to determine if a certain HO criteria is satisfied. The latter is left as an implementation issue to ensure a generic prediction scheme that does not depend on a particular HO model. For instance, the condition of (16) can be used as an example for the HO criteria. The prediction analysis unit confirms/rejects the measurement-based prediction based on the UE HO history and the predicted HO time. Consider  $t_{s,p}$  as the transition probability from the serving DBS<sub>s</sub> to the measurement-based predicted DBS<sub>p</sub>, based on either the crowd behaviour or the individual user behaviour as explained in Section III-B. Define  $t_{min}$  as the minimum HO probability to confirm the prediction from a history perspective. Then the prediction analysis unit confirms the measurement-based prediction if the following condition is true:

$$t_{s,p} \geq t_{min} \quad (20)$$

and it commands the reporting unit to send a PrMR, which contains the predicted DBS along with the predicted remaining time for HO given by (14). Otherwise, the prediction analysis unit rejects the measurement prediction. Notice that the angular span is accounted for in the monitoring and processing phase (i.e.,  $t_{s,p}$  belongs to one of the DBSs that reside within the UE angular span). Fig. 7 provides a flowchart for the operation flow of the prediction analysis unit.

The HO mode decision unit decides the type of HO to be followed by the UE, i.e., predictive or non-predictive HO. In the former, the conventional MRs are suspended, the HO decision and preparation are performed in advance, and HO control is delegated to the UE. It is worth mentioning that the HO mode decision unit can be located at the UE side and integrated with the prediction analysis unit, thus the outcome of the latter implicitly defines the HO type. If the final decision has to be taken based on additional policies defined by the network (i.e., network-controlled UE-assisted decision), then the HO mode decision unit can be moved to the DBS side as shown in Fig. 2.

## V. PERFORMANCE EVALUATION

### A. PREDICTION THRESHOLD ANALYSIS

Fig. 8 shows effect of the UE speed on the expected HO time (in measurement gaps) referenced to the prediction triggering point, with a unified triggering threshold for all users. The considered network parameters are:  $q_s = q_n = 38$  dBm,  $\psi = 130$  m and  $\Delta_g = 200$  ms. A positive  $I_p$  value means that the HO will happen after this value, while a negative  $I_p$  value means a too late prediction (i.e., the HO already happened before the prediction process is triggered). It can be noticed in Fig. 8a that using a unified  $d_{s,thr}$  value for all users could result in a too early prediction especially for

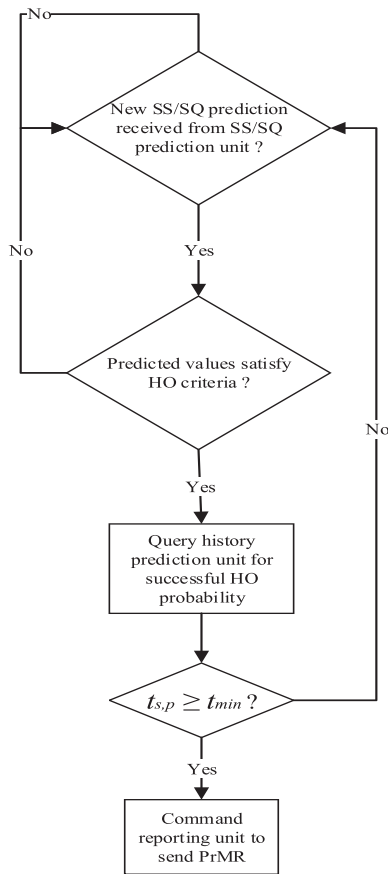


FIGURE 7. Flowchart of the operation flow and decisions of the prediction analysis unit.

low speed users. For instance, with  $d_{s,thr} = 20$  m then a low speed user with  $V = 5$  km/hr will start the prediction process 188 measurement gaps in advance before the actual HO happens. As discussed in Section IV-A and depicted by Fig. 6, such an early prediction has a higher probability of error due to the fact that the prediction precision decreases as the advance period increases. On the other hand, using a large  $d_{s,thr}$  setting of 100 m results in a too late prediction, e.g., with  $V = 5$  km/hr then the prediction process starts after the actual HO happens by 99 measurement gaps.

Fig. 8b indicates that the speed effect on the expected HO time (with a unified triggering threshold) is significantly influenced by the HO hysteresis. It can be seen that increasing the hysteresis  $\Theta$  increases the slope (in absolute value) of the HO time vs speed graph when  $d_{s,thr}$  is constant for all users. This indicates that a low hysteresis setting may be appropriate when  $d_{s,thr}$  is unified for all users. Nonetheless, the HO hysteresis provides other benefits such as delaying the HO to avoid HO ping-pongs and removing the SS/SQ fluctuation effects. As a result, decreasing  $\Theta$  may come at the expense of increasing HO ping-pongs rates.

The observations in Fig. 8 motivate a UE-specific prediction triggering threshold, which is studied in Fig. 9. It can be noticed that  $d_{s,thr,UE}$  is inversely proportional to the UE speed. Expressed differently, low speed users start the

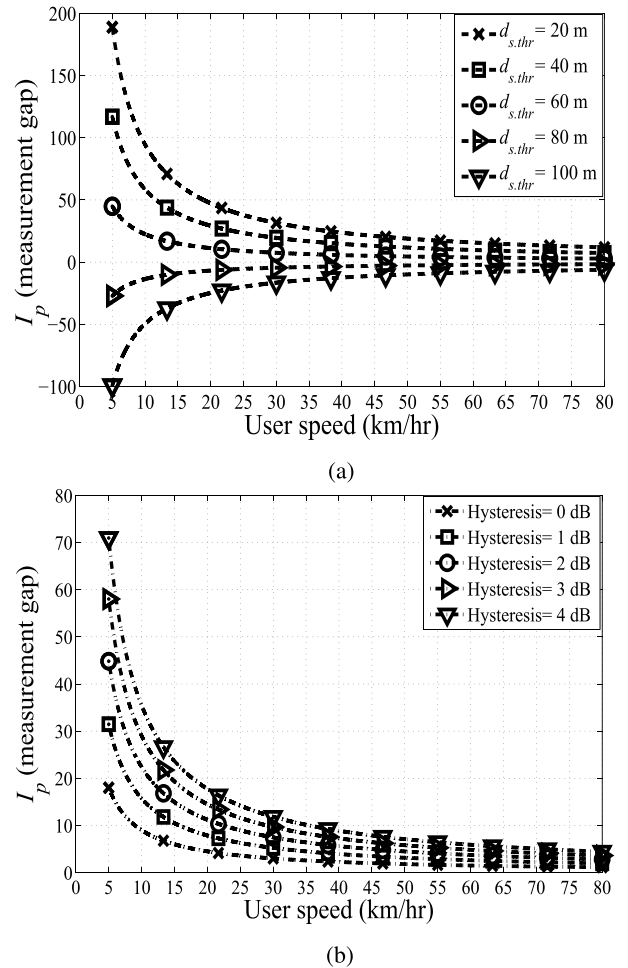


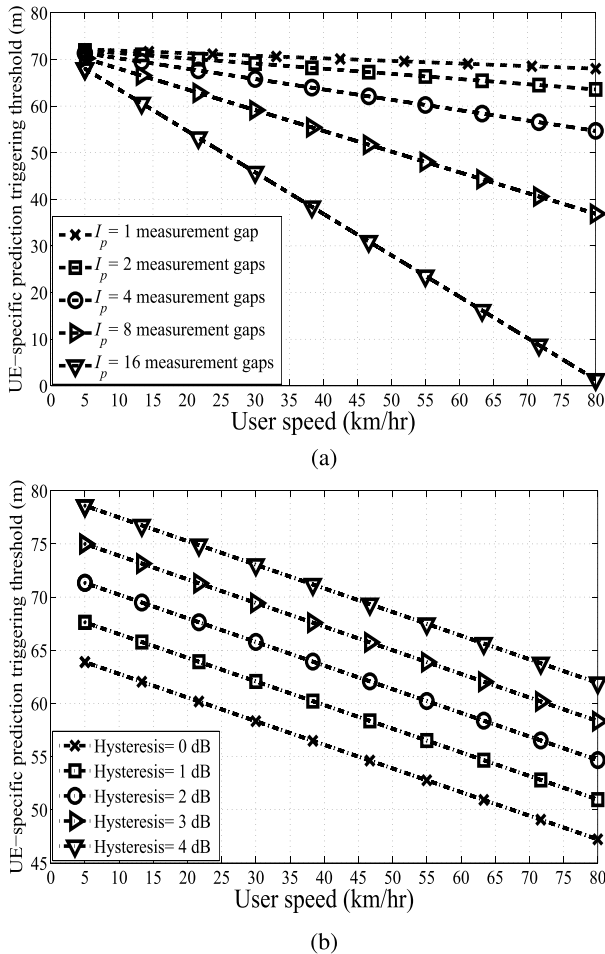
FIGURE 8. User speed vs expected handover time referenced to prediction triggering point with a unified triggering threshold for all users. (a) Effect of  $d_{s,thr}$ , with hysteresis = 2 dB. (b) Effect of hysteresis, with  $d_{s,thr} = 60$  m.

prediction process at a larger distance from the serving DBS as compared with high speed users. This ensures that all users predict the same number of SS/SQ measurements, which in turn allows to set a maximum advance period in order to control the prediction precision and error probability. For example, to ensure that the prediction process does not start more than 8 measurement gaps before the actual HO happens, then a user with  $V = 5$  km/hr and  $V = 80$  km/hr triggers the prediction process at 70 m and 37 m, respectively, from the serving DBS as shown in 9a. Since the expected HO time is inversely proportional to the distance from the serving DBS, then increasing the advance period  $I_p$  reduces  $d_{s,thr,UE}$ . On the other hand, Fig. 9b indicates that the UE-specific  $d_{s,thr,UE}$  and the HO hysteresis have a proportional relationship. This can be linked to the fact that the hysteresis delays the actual HO. Hence, for a fixed advance prediction period target, a higher hysteresis setting increases the required prediction triggering distance from the serving DBS.

B. PREDICTION STATISTICS AND GAINS

System level simulations have been performed to assess performance and gains of the proposed DBS HO scheme.





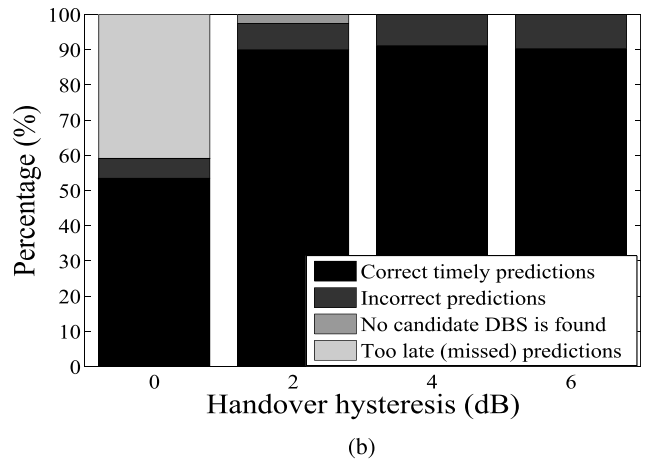
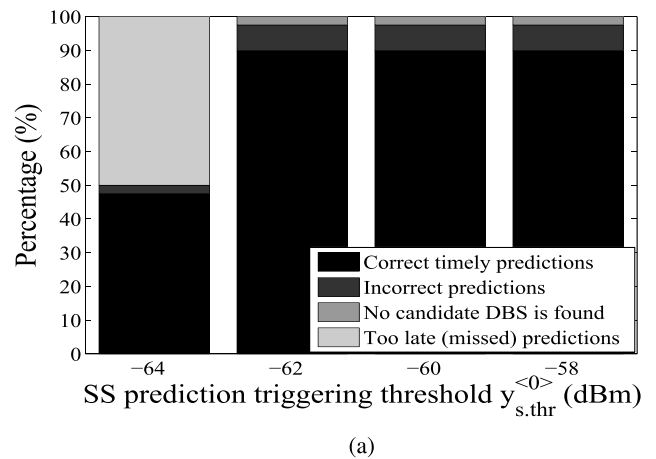
**FIGURE 9.** User speed vs UE-specific prediction triggering threshold. (a) Effect of  $l_p$ , with hysteresis = 2 dB. (b) Effect of hysteresis, with  $l_p = 4$ .

Table 2 provides the considered simulation parameters which are mostly aligned with the 3GPP specifications [14]. Fig. 10 shows prediction accuracy and statistics for several SS triggering thresholds and HO hysteresis values. It can be noticed that this scheme provides a 90% prediction accuracy when  $y_{s,thr}^{(0)} \geq -62$  dBm and HO hysteresis is used (i.e.,  $\Theta > 0$  dB). In addition, it significantly reduces the percentage of incorrect predictions that are not rejected by the prediction analysis unit. Precisely, only 2.5%–9.6% of the predictions resulted in HOs to DBSs other than the actual target DBSs. A very low SS triggering threshold of  $y_{s,thr}^{(0)} = -64$  dBm with a low (or no) HO hysteresis setting results in a significant number of too late predictions. This can be traced to the fact that a low (or no) hysteresis results in an early HO while a low SS triggering threshold delays the prediction process. Expressed differently, in environments/scenarios where HO hysteresis is not used, then the location and span estimation unit needs to be configured to start the prediction process early (i.e., high  $y_{s,thr}^{(0)}$  or small  $d_{s,thr}$  setting).

To evaluate HO latency of the proposed scheme, the approach of [17] has been followed by assuming that the transmission delay for different messages between the

**TABLE 2.** Simulation parameters.

| Parameter           | Value                                   |
|---------------------|---|
| Network layout      | Hexagonal grid, 19 omnidirectional DBSs |
| Inter-site distance | 130 m                                   |
| DBS transmit power  | 38 dBm                                  |
| Transmit mode       | SISO (Single Input Single Output)       |
| User density        | 5 UE/DBS                                |
| User speed          | 10 km/hr for 100% of the users          |
| Channel model       | 3GPP Typical Urban [15]                 |
| Path loss model     | 3GPP Urban [16]                         |
| Frequency           | 2 GHz                                   |
| Bandwidth           | 10 MHz                                  |
| Scheduler           | Round robin                             |
| Measurement gap     | 200 ms                                  |



**FIGURE 10.** Prediction statistics of the measurement-based context-aided predictive DBS handover scheme. (a) Effect of  $y_{s,thr}^{(0)}$ , with hysteresis = 2 dB. (b) Effect of hysteresis, with  $y_{s,thr}^{(0)} = -62$  dBm.

same source-destination pair is the same irrespective of the message size. Similarly, the processing delay for different messages at the same node is constant. In addition, it has been assumed that the mobility management entity (MME) and the serving gateway (S-GW) are located in the same location, thus the transmission delay between these nodes is negligible.

**TABLE 3. Latency values for handover signalling messages.**

| Latency description                       | Value (ms) |
|---|------------|
| Transmission latency between DBSs over X2 | 5          |
| Transmission latency between UE and DBS   | 6.5*       |
| Transmission latency between DBS and MME  | 8.5        |
| Processing latency at DBS                 | 4          |
| Processing latency at MME                 | 5**        |
| Processing latency at S-GW                | 5**        |
| Detach and access latency                 | 12         |

\* Includes processing.

\*\* Does not include UE context retrieval of 10 ms.

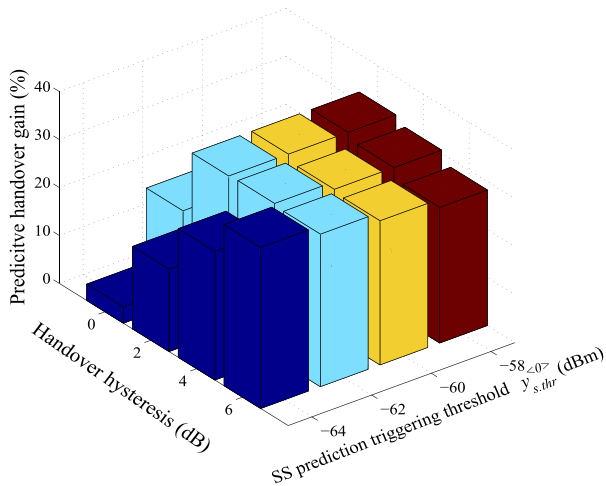


**FIGURE 11. Handover signalling latency reduction.**

Table 3 provides the latency values which are based on the feasibility study reported in [18] for the intra-LTE X2 HO procedure.

Fig. 11 shows gains of the proposed scheme in terms of signalling latency reduction w.r.t. the conventional HO procedure. Based on the latency parameters of Table 3, it can be concluded that the memory-full context-aware predictive HO scheme reduces the DBS HO latency by 33.6% as compared with the conventional HO. Fig. 11 also indicates that the highest gains can be achieved either with a high hysteresis and a low SS/SQ (i.e., a large UE/serving-DBS distance) triggering threshold, or with a low hysteresis and a high SS/SQ (i.e., a small UE/serving-DBS distance) triggering threshold.

It is worth mentioning that the predictive HO scheme proposed in this paper aims to reduce the HO latency rather than reducing the HO signalling overhead (although the periodic MR transmission is suspended in the proposed scheme). This is achieved by exploiting the prediction outcome to perform the HO decision and preparation phases in advance before the HO criteria is met. The gains of this approach in terms of reduction in HO latency are shown and discussed above. However, the HO signalling overhead (after the HO decision) with correct prediction remains the same as the overhead without HO prediction. In the case of incorrect prediction, the HO signalling overhead becomes higher than the overhead without HO prediction. This can be traced to the signalling model where additional messages are needed

**TABLE 4. Normalised predictive handover signalling overhead and latency vs prediction accuracy.**

| Prediction accuracy | Normalised overhead | Normalised latency |
|---------------------|---------------------|--------------------|
| 0%                  | 1.18                | 1.18               |
| 10%                 | 1.16                | 1.12               |
| 20%                 | 1.15                | 1.07               |
| 30%                 | 1.13                | 1.01               |
| 40%                 | 1.11                | 0.96               |
| 50%                 | 1.09                | 0.9                |
| 60%                 | 1.07                | 0.85               |
| 70%                 | 1.05                | 0.79               |
| 80%                 | 1.04                | 0.74               |
| 90%                 | 1.02                | 0.68               |
| 100%                | 1                   | 0.63               |

to cancel the reserved resources at the incorrectly predicted DBS, as can be seen in Fig. 3. To quantify this penalty, Table 4 shows the normalised predictive HO signalling overhead (in terms of the number of the HO-related messages normalised with the number of the HO-related messages in the conventional non-predictive HO scheme), and the normalised predictive HO latency (w.r.t. the conventional HO latency) vs the prediction accuracy.

**VI. CONCLUSION**

Predictive HO signalling at DBS-level is proposed in this paper. With the main objective of minimising the CDSA HO-related RAN signalling latency and monitoring load, a memory-full context-aware predictive DBS HO is proposed. This scheme includes a proactive HO mode selection model to minimise the HO signalling latency, since the predictive HO management strategies may not be suitable in some cases, e.g., unpredictable users with highly random mobility profiles or users visiting new DBSs. Considering the dual connectivity feature of the CDSA, such a predictive approach can be applied with relaxed constraints.

The proposed scheme is operated at the UE, and it predicts the expected HO time in addition to the target DBS. It combines physical proximity (i.e., location information at the UE) to a virtualised UE view of DBS coverage, RF performance derived from SS/SQ measurements, context information and HO history. The SS/SQ measurements are modelled as a time series in a Grey fashion to predict future HO events and the remaining time for HO. In addition, the UE speed and direction are utilised to minimise the storage and processing requirements by narrowing down the candidate DBS set based on the UE angular span. A UE-specific prediction triggering threshold is formulated to improve the measurement prediction precision whilst minimising the UE processing load. For a certain advance prediction period (and hence a certain precision target), it has been found that the UE-specific triggering threshold is inversely proportional (in distance format) and directly proportional (in SS/SQ format) to the UE speed. The switching point between predictive and conventional HO procedures is defined based on the successful HO probability which is obtained from the history

prediction model.

Simulation results show that the proposed predictive scheme reduces the HO signalling latency by 33.6% as compared with the conventional LTE X2 HO procedure. These gains depend on network-defined HO parameters such as the HO hysteresis and transmit power, in addition to the UE-specific prediction parameters such as the prediction triggering threshold. This suggests an appropriate setting of both the network-defined and the UE-specific parameters to achieve the maximum gain.

## ACKNOWLEDGMENT

The authors would like to acknowledge the support of the University of Surrey 5GIC members (<http://www.surrey.ac.uk/5gic>).

## REFERENCES

- [1] J. G. Andrews et al., "What will 5G Be?" *IEEE J. Sel. Areas Commun.*, vol. 32, no. 6, pp. 1065–1082, Jun. 2014.
- [2] Nokia Siemens Networks, "2020: Beyond 4G, radio evolution for the gigabit experience," Nokia Siemens Networks, Espoo, Finland, White Paper C401-00722-WP-201106-1-EN, Aug. 2011. [Online]. Available: <http://nsn.com/file/15036/2020-beyond-4g-radio-evolution-for-the-gigabit-experience>
- [3] *Evolved Universal Terrestrial Radio Access (E-UTRA); Mobility Enhancements in Heterogeneous Networks, Version 11.1.0 Release 11*, document 3GPP TR 36.839, Dec. 2012. [Online]. Available: <http://www.3gpp.org/DynaReport/36839.htm>
- [4] A. Mohamed, O. Onireti, M. A. Imran, A. Imran, and R. Tafazolli, "Control-data separation architecture for cellular radio access networks: A survey and outlook," *IEEE Commun. Surveys Tuts.*, vol. 18, no. 1, pp. 446–465, 1st Quart., 2015.
- [5] *Study on Scenarios and Requirements for Next Generation Access Technologies, Version 0.4.0 Release 14*, document 3GPP TR 38.913, Jun. 2016. [Online]. Available: <http://www.3gpp.org/DynaReport/38913.htm>
- [6] H. Ishii, Y. Kishiyama, and H. Takahashi, "A novel architecture for LTE-B: C-plane/U-plane split and phantom cell concept," in *Proc. IEEE Globecom Workshops*, Dec. 2012, pp. 624–630.
- [7] X. Xu, G. He, S. Zhang, Y. Chen, and S. Xu, "On functionality separation for green mobile networks: Concept study over LTE," *IEEE Commun. Mag.*, vol. 51, no. 5, pp. 82–90, May 2013.
- [8] A. Mohamed, O. Onireti, M. A. Imran, A. Imran, and R. Tafazolli, "Predictive and core-network efficient RRC signalling for active state handover in RANs with control/data separation," *IEEE Trans. Wireless Commun.*, vol. 16, no. 3, pp. 1423–1436, Mar. 2017.
- [9] A. Mohamed, O. Onireti, S. A. Hosenitabatabae, M. Imran, A. Imran, and R. Tafazolli, "Mobility prediction for handover management in cellular networks with control/data separation," in *Proc. IEEE Int. Conf. Commun. (ICC)*, Jun. 2015, pp. 3939–3944.
- [10] *Evolved Universal Terrestrial Radio Access (E-UTRA); Radio Resource Control (RRC) Protocol Specification, Version 13.1.0 Release 13*, document 3GPP TS 36.331, Apr. 2016. [Online]. Available: [http://www.etsi.org/deliver/etsi\\_ts/136300\\_136399/136331/13.01.00\\_60/ts\\_136331v130100p.pdf](http://www.etsi.org/deliver/etsi_ts/136300_136399/136331/13.01.00_60/ts_136331v130100p.pdf)
- [11] J. L. Deng, "Introduction to Grey system theory," *J. Grey Syst.*, vol. 1, no. 1, pp. 1–24, 1989.
- [12] H. Hu, J. Zhang, X. Zheng, Y. Yang, and P. Wu, "Self-configuration and self-optimization for LTE networks," *IEEE Commun. Mag.*, vol. 48, no. 2, pp. 94–100, Feb. 2010.
- [13] M. Amirijoo, P. Frenger, F. Gunnarsson, H. Kallin, J. Moe, and K. Zetterberg, "Neighbor cell relation list and physical cell identity self-organization in LTE," in *Proc. IEEE Int. Conf. Commun. (ICC)*, May 2008, pp. 37–41.
- [14] *Physical Layer Aspects for Evolved Universal Terrestrial Radio Access (UTRA), Version 7.1.0 Release 7*, document 3GPP TR 25.814, Sep. 2006. [Online]. Available: <http://www.qtc.jp/3GPP/Specs/25814-710.pdf>
- [15] *Deployment Aspects, Version 13.0.0 Release 13*, document 3GPP TR 25.943, Jan. 2016. [Online]. Available: <http://www.3gpp.org/DynaReport/25943.htm>
- [16] *Evolved Universal Terrestrial Radio Access (E-UTRA); Radio Frequency (RF) System Scenarios, Version 13.0.0 Release 13*, document 3GPP TR 36.942, Jan. 2016. [Online]. Available: <http://www.3gpp.org/dynareport/36942.htm>
- [17] L. Wang, Y. Zhang, and Z. Wei, "Mobility management schemes at radio network layer for LTE femtocells," in *Proc. IEEE 69th Veh. Technol. Conf. (VTC)*, Apr. 2009, pp. 1–5.
- [18] *Feasibility Study for Evolved Universal Terrestrial Radio Access (UTRA) and Universal Terrestrial Radio Access Network (UTRAN), Version 11.0.0 Release 11*, document 3GPP TR 25.912, Oct. 2012. [Online]. Available: <http://www.3gpp.org/DynaReport/25912.htm>



**ABDELRAHIM MOHAMED** (S'15–M'16)

received the B.Sc. degree (Hons.) in electrical and electronics engineering from the University of Khartoum, Sudan, in 2011, and the M.Sc. degree (Hons.) in mobile and satellite communications and Ph.D. degree in electronics engineering from the University of Surrey, U.K., in 2013 and 2016, respectively. He is currently a Post-Doctoral Research Fellow with the ICS/5GIC, University of Surrey, Surrey, U.K. He is currently involved in the

RRM, MAC, and RAN Management work area, and the New Physical Layer work area in the 5GIC with the University of Surrey. He is also involved in the energy proportional eNodeB for LTE-Advanced and Beyond project, the planning tool for 5G network in mm-wave band project, in parallel to working on the development of the 5G system level simulator. His research contributed to the QSON project and the FP7 CoRaSat Project. His main areas of research interest include radio access network design, system-level analysis, mobility management, energy efficiency, and cognitive radio. He secured first place and top ranked from the Electrical and Electronic Engineering Department, University of Surrey, during his M.Sc. studies. He was a recipient of the Sentinels of Science 2016 Award.



**MUHAMMAD ALI IMRAN** (M'03–SM'12)

received the B.Sc. degree (Hons.), and the M.Sc. (Hons.) and Ph.D. degrees from Imperial College London, U.K., in 2002 and 2007, respectively. He was a Visiting Professor with the 5G Innovation Centre, University of Surrey, U.K., from 2007 to 2016. He is currently a Professor in communication systems with the University of Glasgow, the Vice Dean with Glasgow College, UESTC, and the Program Director of Electrical and Electronics with Communications. He is currently also an Adjunct Associate

Professor with the University of Oklahoma, USA. He has led a number of multimillion-funded international research projects encompassing the areas of energy efficiency, fundamental performance limits, sensor networks, and self-organising cellular networks. He also led the new physical layer work area for 5G Innovation Centre, Surrey. He has a global collaborative research network spanning both academia and key industrial players in the field of wireless communications. He has supervised 21 successful Ph.D. graduates and published over 200 peer-reviewed research papers including over 20 IEEE Transaction papers. He secured first rank in his B.Sc. degree and a distinction in his M.Sc. degree along with an award of excellence in recognition of his academic achievements conferred by the President of Pakistan. He is a Senior Fellow of Higher Education Academy, U.K. He was a recipient of the IEEE Comsoc's Fred Ellersick award 2014, Sentinel of Science Award 2016, FEPS Learning and Teaching award 2014, and twice nominated for Tony Jean's Inspirational Teaching award. He is a shortlisted finalist for The Wharton-QS Stars Awards 2014, Reimagine Education Award for innovative teaching, and VC's learning and teaching award in University of Surrey. He has given an invited TEDx talk (2015) and over ten plenary talks, several tutorials, and seminars in international conferences and other institutions. He has taught on international short courses in USA and China. He is the Co-Founder of the IEEE Workshop BackNets 2015 and chaired several tracks/workshops of international conferences. He is an Associate Editor for the IEEE COMMUNICATIONS LETTERS, the IEEE OPEN ACCESS and *IET Communications Journal*.



**PEI XIAO** (SM'11) is currently a Professor with the Home of 5G Innovation Centre (5GIC), Institute for Communication Systems, University of Surrey. He is currently the Technical Manager of 5GIC, leading the research team at on the new physical layer work area, and coordinating/supervising research activities across all the work areas within 5GIC. Prior to this, he was with Newcastle University and Queen's University Belfast. He also held positions at Nokia Networks in Finland. He has published extensively in the fields of communication theory and signal processing for wireless communications.



**RAHIM TAFAZOLLI** (SM'09) is currently a Professor and the Director with the Institute for Communication Systems and the 5G Innovation Centre, University of Surrey, U.K. He has authored over 500 research papers in refereed journals, international conferences, and as an invited speaker. He is the Editor of two books on *Technologies for Wireless Future* (Wiley) Vol.1 in 2004 and Vol.2 2006. He was appointed as Fellow of Wireless World Research Forum in 2011, in recognition of his personal contribution to the wireless world. As well as heading one of Europe's leading research groups.

• • •